Spacecraft, Vol. 27, No. 1, 1990, pp. 9-14.

[8] Landrom, D.B., DeJarnaette, F.R., and Boman, B.L., "Engineering Method for Calculating Surface Pressures and Heating Rates on Vehicles With Embeded Shocks", Journal of Spacecraft and Rockets, Vol. 29, No.6, 1992, pp. 756-764.

[9] Zoby, E.V., and Simmonds, A. L.,"Engineering Flowfied Method With Angle-of- Attack Applications", Journal of Spacecraft, Vol. 22, No.4, 1985, pp. 398-404.

[10] Rakich, J.V., and Lanfranco, M.J., "Numerical Computtion of Space Shuttle Laminar Heating and Surface Stramlines", Journal of Spacecraft , Vol.14, No. 5, 1977, pp. 265-272.

[11] Riley, C.J., and DeJarnette, F.R., "Engineering Aerodynamic Heating Method for Hypersonic Flow", Journal of Spacecraft and Rockets, Vol. 29, No. 3, 1992, pp. 327-334.

[12] Riley, C.J., and DeJarnette, F.R., "Engineering Calculations of Three-Dimensional Inviscid Hypersonic Flowfields", Journal of Spacecraft, Vol. 28, No. 6, 1991, pp. 628-635.

[13] Zoby, E.V., and Thompson, R.A., "Flowfield and Vehicle Parameter Influence on Hypersonic Heat Transfer and Drag", Journal of Spacecraft Vol. 27, No. 4,1990, PP. 361-368.

[14] Maslen, S. H.,"Invisid Hypersonic Flow Past Smooth Symmetric Bodies", AIAA Journal, Vol. 2, No. 6, 1964, pp. 1055-1061.

[15] Maslen, S.H., "Asymmetric Hypersonic Flow ", NASA CR-2123, Sept. 1972.

[16] Riley, C.J., "An Engineering Method for Interactive Inviscid-Boundary Layers in Three-Dimensional Hypersonic Flow", Ph.D. Thesis,Dept. of Mech. and Aerospace Eng., North Carolina State University , 1992.

[17] Van Dyke, M.D., and Gordon, H.D., "Supersonic Flow past a Family of Blunt Axisymmetric Bodies", NASA TR R-1, 1959.

[18] Billig, F.S., "Shock-Wave Shapes Around Spherical - and Cylindrical-Nosed Bodies", AIAA Journal, Vol. 5, No. 9, 1967, pp. 1557-1562.

[19] Hornbeck, R.W., "Numerical Methods", Prentice-Hall, Inc. Englewood Cliffs., New Jersey 07632, 1975.

[20] Riley, C. J., "An Approximate Method for Calculating Inviscid Flowfields Over Three-Dimensional Blunt-Nosed Bodies in Hypersonic Flow", M.Sc. Thesis, Dept. of Mech. and Aerospace Eng., North Carolina State University, **1988.**

[21] Morrison, A. M., Solomon, J. M., Ciment , M., and Fergusen, R.E., "Handbook of Sphere-Cone Flowfields and Pressure Distributions: Volume I", **NSWC/WOL/TR 75-45, Dec. 1975.**

[22] Miller III, C.G., "Measured Pressure Distributions, Aerodynamic Coefficients, and Shock Shapes on Blunt Bodies at Incidence in Hypersonic Air and CF4", NASA TM-84489, Sept. 1991.

[23] Weilmuenster, K. J., and Hamilton, H.H., "Calculations of Inviscid Flow Over Shuttle-Like Vehicles at High Angles of Attack and Comparisons With Experimental Data", NASA TP-2103, May 1983.

[24] Marconi, F., Salas, M., and Yaeger, L., " Development of a Compurter Code For Calculating the Steady Super/Hypersonic Inviscid Flow around Real Configurations. Vol. I-Computational Technique", NASA CR-2675, April 1976.

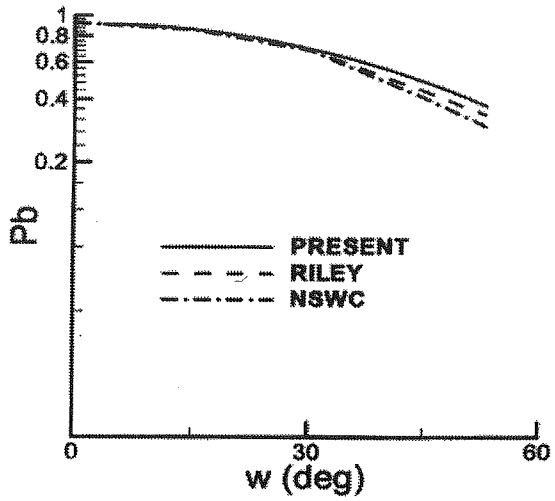

Figure (11) Variation of surface pressure with surface angle; Minf=20.

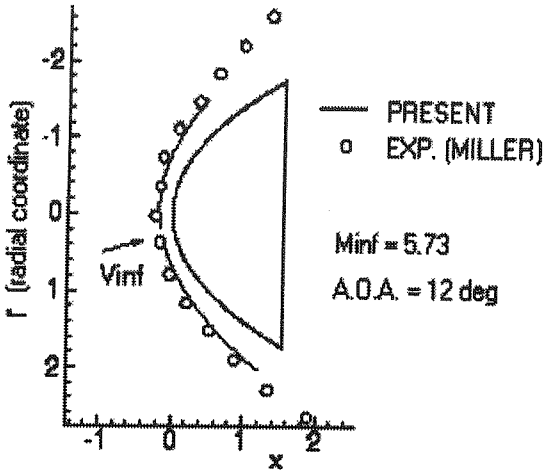

Figure (13) Shock shape comparison in plane of symmetry.

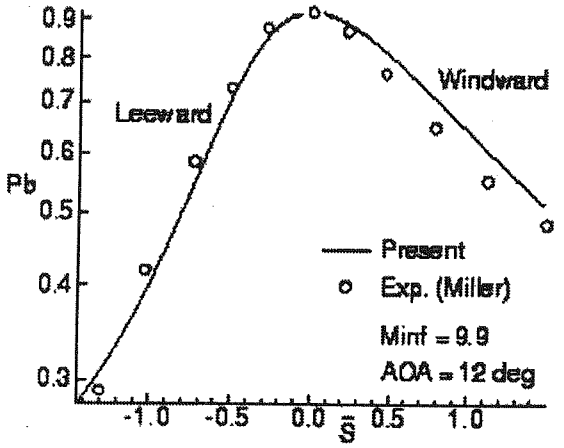

Figure (12) Surface pressure variation in plane of symmetry.

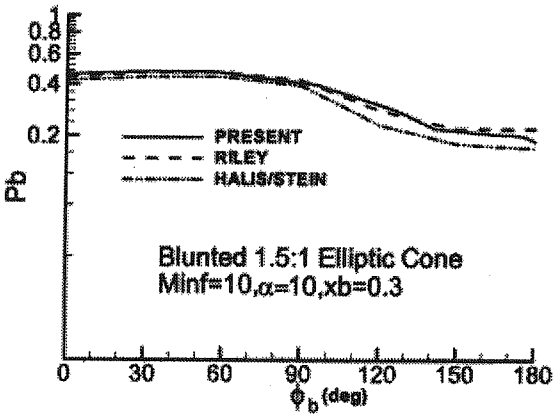

Figure (14) Surface pressure variation in circumferential direction.

Refrences

[1] Anderson, J.D., " Hypersonic And High-Temperature Gas Dynamics", McGraw-Hill Book Co., 1989, Chap. 6.

[2] Zoby, E.V., Moss, J,N., and Sutton, K., "Approximate Convecting Heating Equations for Hypersonic Flows", Journal of Spacecraft, Vol. 18, No. 1,1981, pp.64-70.

[3] Hamilton, H.H., DeJarnette, F.R., and Weilmuenster, K.J., "Application of Axisymmetric Analog for Calculating Heating in Three-Dimensional Flow", Journal of Spacecraft, Vol.24, No.4, 1987, pp. 296-302.

[4] Hoffmann, K. A., Wilson, D.F., and Hamburger, C., "Aerothermodynamic Analysis of projectiles at Hypersonic Speeds", AIAA Paper 89-2185-CP,1989.

[5] DeJarnette, F.R., Hamilton, H.H., Weilmuenster, K.J., and Cheatwood, F.M., "A Review of Some Approximare Methods Used in Aerodynamic Heating Analysis", Journal of Thermophysics, Vol.1, No. 1. 1987, pp. 5-12.

[6] Dejarnette, F.R., and Hamilton, H.H., "Inviscid Surface Streamlines and Heat Transfer on Shuttle-Type Configurations", Journal of Spacecraft Vol.10, No. 5,1973, pp. 314-320.

[7] Riley, C. J., DeJarnette, F.R., and Zoby, E.V., "Surface Pressure and Streamline Effects on Laminar Heating Calculations", Journal of

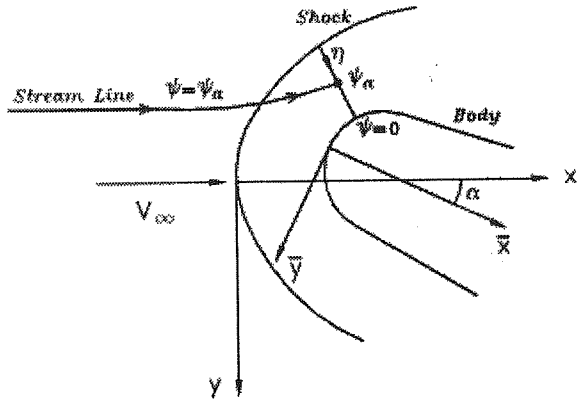

Figure (5) Shock and body axes.

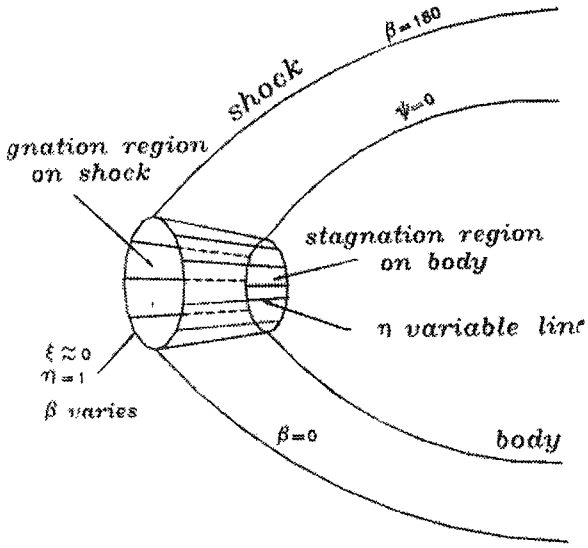

Figure (6) Curvlinear coordinates at stagnation region.

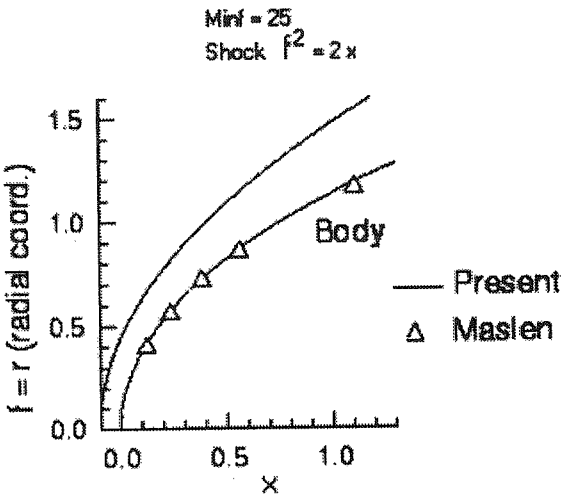

Figure (7) Calculated body comparison for a parabolic shock.

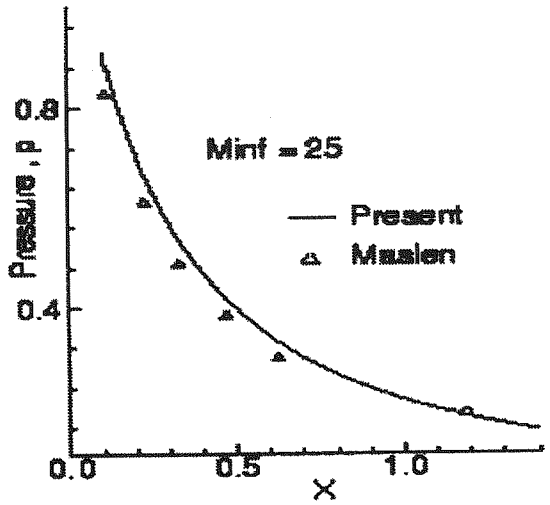

Figure (8) Pressure comparison along the calculated body for a parabolic shock.

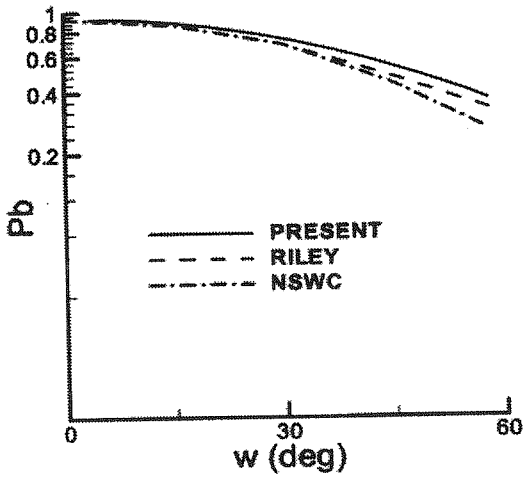

Figure (9) Variation of surface pressure with surface ngle; Minf=5.

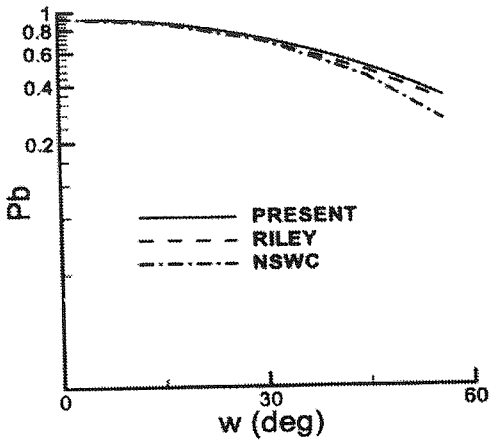

Figure (10) Variation of surface pressure with surface angle; Minf=10.

Example 4:

In this example we will consider an asymmetric body of elliptic cone with b=1, cone half angle of 10.26 degrees in the windward plane , and an ellipticty of 1.5, i.e. $\overline{B}$=2.25. Starting from an initial shock wave, 24 iterations were required to converge the subsonic - transonic solution for a region with M ≤ 1.05. This took about 105 seconds on a pentium-200. Circumferential surface pressure distribution at an axial location of $\overline{x}$=0.3 is compared with the results of computer codes HALIS[23] and STEIN[24] , and results of Ref.16. The agreement is unexpectedly very good. Present results match the results of Ref. 16 very well. In comparison to HALIS/STEIN results, the higher prediction of present algorithm is in the same order of the prediction of Ref.16; otherwise the overal prediction is impressing.

Having presented the above examples it can be concluded that the present algorithm is capable of predicting inviscid flowfields around hypersonic body noses with different geometries at angle of attack. In all cases very good results were predicted when comparing with experimental data and other numerical results. The method is an approximate engineering one and the accuracy of its results should be analyzed in this context and the fact that its computer costs are very low.

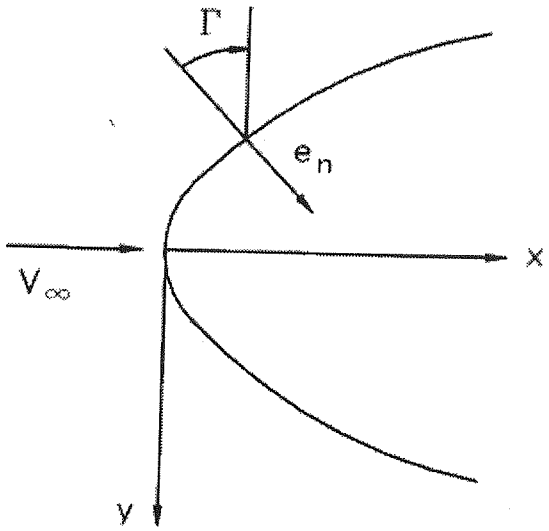

Figure (1) Side view of shock wave geometry.

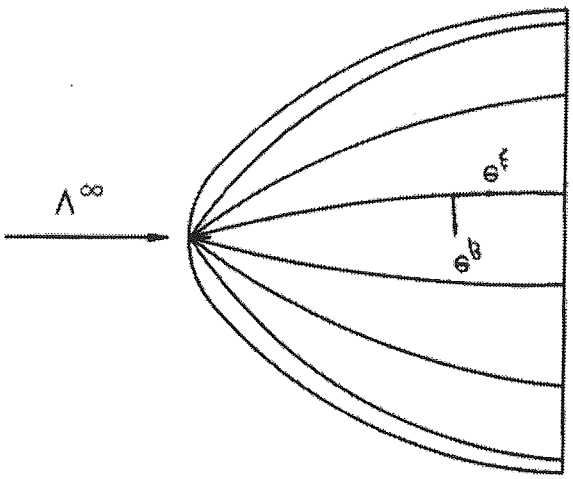

Figure (3) Side view of shock-oriented curvilinear coordinate system.

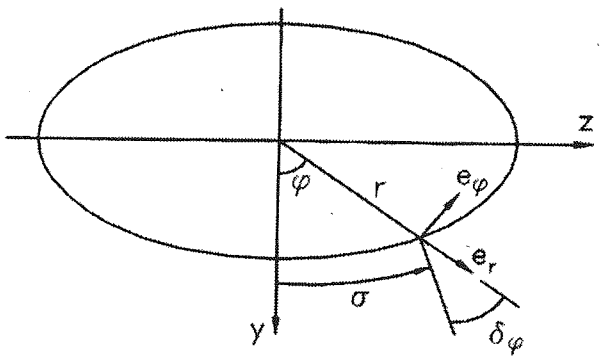

Figure (2) Rear view of shock wave geometry.

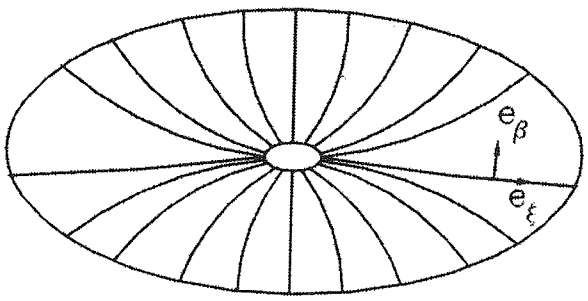

Figure (4) Front view of shock-oriented curvilinear coordinate system.

Example 2:

Consider a spherical nose at zero angle of attack. The inviscid flowfield around this nose is solved for free stream Mach numbers of 5, 10, and 20. Solution domain of this symmetric flow includes the subsonic-transonic region where $M_\infty \leq 1.2$ For the mentioned Mach numbers, the following figures were observed. Number of iterations needed for shock - shape correction were 20, 10, and 11, respectively. Number of points along the surface (i.e. in ξ direction) were 53, 52,juand 51, respecvtively, and CPU time of execution on a pentium-200 were 38, 22, and 23 seconds, respectively. Pressure distributions along the surface from stagnation point to the end of solution domain are plotted against the results of Ref. 20 (Riley) and the finite-difference Euler code of NSWC[21] in Figs. 9, 10, and 11. In these figures p_b is the surface pressure and w indicates the position angle of a point along the surface. As seen surface Mach number of 1.2 occurs at w =57.9, 56.0, and 53.14 in these figures, respectively. The agreement between the present results and those of Ref.20 is generally good. Both of these results have predicted higher pressures in comparison to the prediction of NSWC code. However, as an approximate method which has the advantage of being economic and very fast in terms of computer performance, the present results have excellent accuracy. Note that results of Ref. 20 lie some where between the present results and the experimental data. It should be mentioned that approximate methods perform better when the shock layer is thinner. Therefore at M_∞ =5, it has cost more iterations and CPU time for solution convergence.

Example 3:

In this case an axisymmetric paraboloid at 12 deg. angle of attack is experiencing free stream Mach number of 9.9. Starting with an initial shock shape, the fully three-dimensional subsonic-transonic flowfied around the body is obtained after 15 iterations of shock- shape correction. With pentium - 100 processor this computation took less than two minutes. The only available data for comparison is the pressure distribution along the surface in plane of symmetry; this is shown in Fig. 12. As seen comparison is made with the experimental data of Ref.22. In this figure, $\bar{z}$ is the distance along the surface starting from the stagnation point. In the leeward section the agreement with experiment is very good. In the windward section, however, present method has predicted pressure higher than that of experiment . However, the agreement is still good since we are comparing our results with experiment.

To compare the shape of shock wave produced by such a paraboloid body, free stream Mach number is changed to 5.73 for which experimental data are available in literature. Comparison of shock shape with the experimental data of Ref.22 is presented in Fig.13. As seen, the agreement with the results of Ref.22 is very good; although the present method has predicted a shock wave which is a bit closer to the body. In this case 18 iterations were performed in less than 2.5 minutes to determine the correct shock wave and its fully 3D flowfield for the paraboloid at M_∞=5.73. Again, note that more efforts are spent at lower Mach numbers. It is noted that the iteration procedure implemented in this paper is more simple than that of Refs. 11 and 12, however the number of iterations needed for convergence is higher than those given in these references.

calculations.

Note that this is the procedure for subsonic transonic region. Although there is no limitation to apply the above procedure in supersonic region, a space marching approach is more convinient and easy to apply in this region. This is not considered in this paper. Finally we mention that the variables are nondimensionalized as given bellow

$$L=\frac{L'}{L'_r} \qquad \psi=\frac{\psi'}{\rho'_\infty V'^2_\infty L'^2_r}$$

$$V=\frac{V'}{V'_\infty} \qquad \rho=\frac{\rho'}{\rho'_\infty}$$

$$p=\frac{p'}{\rho'_\infty V'^2_\infty} \qquad h=\frac{h'}{V'^2_\infty}$$

$$T=\frac{T'}{T'_\infty} \qquad R=\frac{R'T'_\infty}{V'^2_\infty}$$

where prime denotes dimensionalized variables, subscript ∞ indicates free stream, and L represents the reference length.

4-Results

In this section numerical results obtained by the present method are compared with those obtained from experiment and other numerical results. A as was mentioned before we are using an inverse method. Therefore the flowfield behind a given shock wave is first solved to obtain the corresponding body shape. Since this body shape will not match usually the shape of real body, a process of repeating shock-shape correction and solving the flowfield behind of it is continued until the calculated body matches the real one. Therefore, the first example chosen in this paper is to evaluate the algorithm for the first part of the above process.

Example 1:

Consider a symmetric shock shape of f=2x. Angle of attack is zero and M_∞=25. Twenty one points are chosen in the direction of normal to the shock wave. Along the shock line, i.e. ξ direction, position of points depends on the accuracy chosen in the variable step-size integration of six variables. Integration steps are small at the front of shock wave since it is higly curved in this region. For the same accuracy, larger steps are taken at the downstream of the shock. On a computer with pentium-100 processor it took less than 10 seconds to calculate flowfield between the shock wave and its corresponding body (the resulted body with ψ=0). In Fig. 7, the body shape calculated by the present method is compared with the one obtained in Ref. 14. The agreement is excellent. Figure 8 demonstrates the good agreement that exists between the two pressure distributions. The small difference between the results is because Ref.14 calculates pressure from a formulation excluding a (η^2-1) term given in Eq. (10); it is expected that pressure distribution of the present method would be more accurate.

In next examples, inviscid flowfield is solved around several 3D bodies. Obviously our test cases would be limited to cases whose results are available in the literature of approximate engineering methods. In all of the following examples 21 points are chosen in direction of η between the shock and body, and the circumferential direction of β =0° to β=180° is subdivided into 18 sections (i.e.19 points).

$$h_\beta = \alpha \frac{yz}{(B^2y^2 + z^2)^{0.5}} \quad (28)$$

$$\psi_s = \alpha \frac{yz}{B+1} \quad (29)$$

where

$$\alpha = \frac{1}{\sin\beta\cos\beta}\left(\frac{B^2\cos^2\beta+\sin^2\beta}{B\cos^2\beta+\sin^2\beta}\right) \quad (30)$$

With these shock line variables at each β, values of p, u, v, ρ, and enthalpy, $\hat{h}$, are calculated for different values of η along a line normal to the shock; see Fig.6. Shock stand-off distance is also calculated for each β at x_ε. All of these quantities are computed using limiting form of Eqs. (10-14); see Ref. 16.

4) Since the initial values of shock line variables are known, Eqs. (21-23) can be integrated to obtain their values for different ξ along the three β constant lines. It is obvious that when these values are determined at each ξ and β, Eqs. (10-14) should be used to calculate shock stand-off distance, n_b. Therefore by marching along β constant lines all of the flow variables and gemetric values have been determined for shock layer under these three shock lines. Marching procedure is stopped, whenever at the calculated body (where $\psi = 0$), surface Mach number becomes supersonic on β constant lines.

5) Having known $n_b(\xi, \beta)$ at all ξ along the three β constant lines, the calculated body shape for the assumed shock wave has been already specified. It remains to compare this calculated body shape with the shape of the given body. Based on a defined error, if these two bodies match each other the guessed shock shape would be the one that will be produced by the given (real) body Otherwise the shock shape should be so corrected that it results in a calculated body with less miss - match. Since the shock shape is generated by six parameters, six equations are required for calculation of new parameters. The procedure is as follows

a) At the end of three shock lines of β=0°, 90°, 180°, errors in body position and its slope are estimated as

$$e_{1j} = \left(\frac{n_b - n_{b_{geo}}}{n_{b_{geo}}}\right)_{(ie)_j}$$

$$e_{2j} = \left(\frac{\nabla n_b - \nabla n_{b_{geo}}}{\nabla n_{b_{geo}}}\right)_{(ie)_j} \quad (31)$$

in which subscripts *geo* and *ie* indicate real body and the last integration point on the shock lines, respectively, *j* represents the shock line number, and —is backward differencing operator along b constant lines.

b) Based on these errors new positions and slopes are estimated at the last integration points of the three shock lines.

c) Imposing these six conditions to shock shape equation of (16), results in a nonlinear system of six algebraic equations. New values of shock shape parameters b_1, b_2, b_3, c_1, c_2, and d_1 are obtained by iteratively solving this system of equations. With these values steps of 2 to 5 are repeated until the six shock parameters remain unchanged within a defined tolerance. Now , since the right shock shape for the given body nose is specified, one can repeat steps 2 to 4 for a number of β constant lines (e.g. 19 lines) to determine the whole solution domain between shock and body; this will be needed later for supersonic flow

$$\frac{\partial \sin \Gamma}{\partial s} = - K_{\xi} \cos \Gamma \qquad (23)$$

where $\frac{\partial}{\partial s} = \frac{1}{h_{\xi}} \frac{\partial}{\partial \xi}$. The above equations are obtained using Eqs. (1) and (7), and relations transforming coordinates between cylindrical and curvilinear systems [16]. Values of p_1, p_2 and v_1 should be also calculated since they are defined at the shock surface by Eq. (12). Note that as is seen in Figs. 3 and 4 a shock line is formed from intersection of a β-constant line with shock surface. Equations (21-23) are reported in Ref. 12; however in this reference instead of s, integration variable of x is used. Due to this replacement the first P.D.E. in Eqs. (21) is eliminated, and right-hand-side of other five equations are divided by cosΓ. Note that for axisymmetric flow only one shock line is needed.

The integration is performed numerically using a variable-step size, second-order, predictor-corrector scheme [19]. In this scheme, shock line variables at location i, representing current ξ, are calculated using their values at two previous locations *i*-1 and *i*-2. Predicted and corrected values at i are compared with each other. If the error is less than a prescribed value, the step size Δξ (or Δs) is acceptable, otherwise the step size is varied until the above criterion is met. Note that the above scheme can be started from *i*=3, and for *i*=2 a second-order Runge-Kutta scheme may be used. Reference 16 has proposed to transfer s, the distance along a shock line, to a time-like variable, *t*, so that at each integration step the same axial location is ensured for all shock lines. This transformation relation is

$$\frac{\partial}{\partial t} = \frac{x}{\cos \Gamma} \frac{\partial}{\partial s} \qquad (24)$$

We have adopted the above transformation since it makes the numerical calculation of other derivatives (specially in ϕ direction) convenient .

3) Integration cannot be started from stagnation point, i.e. ξ =0, since this point is a singular point. Therefore using limiting form of shock shape given by Eqs. (15-18) at stagnation region, i.e. $\xi \rightarrow 0$, initial values of shock line variables x, r, ϕ, Γ, h_{β}, and ψ_s will be determined for all shock lines originating from this region (at this stage only three of them). A limiting from of shock shape could be an elliptic paraboloid as

$$By^2 + z^2 = 2cx$$

where

$$c = R_z \qquad B = \frac{R_z}{R_y} \qquad (25)$$

and R_y and R_z are shock radii of curvature at the origin in x-y and x-z planes, respectively. By choosing a small value for ε, x-coordinate is determined for stagnation region using

$$\varepsilon^2 = 2cx_{\varepsilon} \qquad (26)$$

where subscript ε indicates initial values at stagnation region . Although in Ref. 16 a value between 0.01 and 0.1 is proposed for ε, our experience is that values around 0.03 work very well. As before $\beta = \phi_{\varepsilon}$, and therefore ϕ_{ε} is determined for each of the three shock lines. Using Eq. (25) r_{ε} and therefore y_{ε} and z_{ε} are determined for each β. Continuing derivation of other shock line variables of Γ, h_{β} and ψ_s, the following expressions can be obtained for the limiting case of stagnation region based on their definitions.

$$\tan \Gamma = \frac{c}{(B^2 y^2 + z^2)^{0.5}} \qquad (27)$$

$$\tilde{D}(x)=f_2^2 \qquad (17)$$

Note that $f(x,\phi)$ is radial coordinate of the 3D shock surface in shock cylindrical coordinate system. The three longitudinal conic sections are introduced as

$$f_k^2+b_k x^2-2c_k x+2d_k x f_k=0 \qquad k=1,2,3 \qquad (18)$$

where k represents shock profiles for $\phi = 0°$, 90° and 180°, respectively. This shock shape has the limitation of not allowing inflections in the axial direction. Therefore sonic line should remain on the blunted nose of body. The shock shape, defined above includes nine parameters of b_k, c_k and d_k where k=1, 2, 3. For a shock wave with continuous curvature at the origin in the plane of symmetry c_1 should be equal to c_3.

Additional constraints on coefficients d_k, which are $d_2 = 0$ and $d_1 = -d_3$ imply that the shock would be symmetric with respect to x-y plane. Therefore, angle of attack is only defined in the x-y plane. With these constraints the number of parameters reduces to six.

3-SOLUTION PROCEDURE

In this section, the iteration procedure for determining six parameters of b_1, b_2, b_3, c_1, c_2, and d_1 is introduced. These parameters define the shock shape that will be formed ahead of a body nose with the following formulation

$$\bar{r}=\bar{f}(\bar{x},\bar{\phi}) \qquad (19)$$

where

$$\bar{f}^2(\bar{B}\cos^2\bar{\phi}+\sin^2\bar{\phi})=2\bar{x}-\bar{b}\bar{x}^2 \qquad (20)$$

in which $\bar{r},\bar{x},\bar{\phi}$ are the body-cylindrical coordinates. Figure 5 demonstrates positions of shock and body axes with respect to each other. In this equation, the non-dimensional nose radius in $\bar{x}$-$\bar{z}$ plane is equal to unity. Parameter $\bar{B}$ governs the ellipticity of the body cross section; $\bar{B}$ = (ellipticity)^2. The parameter $\bar{b}$ determines the longitudinal shape of the body. An ellipsoid is produced if $\bar{b} \geq 0$, and a paraboloid is generated if $\bar{b}$ =0. For determination of shock wave parameters following steps should be taken. Note that in this procedure flowfield is also solved behind the shock wave.

1) Initial values are guessed for the above six parameters. For an axisymmetric flow these six parameters reduce to b_1 and c_1. Better values can be guessed using Ref. 18.

2) By moving along three shock lines of β=0°,90°, and 180°, extending from stagnation region to the end of subsonic region, shock line variables of x, r, ϕ, Γ, h_β, and ψ_s are calculated at each ξ. These calculations are performed by integrating the following partial differential equations along the three shock lines.

$$\frac{\partial x}{\partial s}=\cos\Gamma$$

$$\frac{\partial r}{\partial s}=\sin\Gamma\cos\delta_\phi$$

$$\frac{\partial \phi}{\partial s}=-\frac{\sin\Gamma\cos\delta_\phi}{r} \qquad (21)$$

$$\frac{\partial h_\beta}{\partial s}=h_\beta k_\beta \tan\Gamma$$

$$\frac{\partial \psi_s}{\partial s}=h_\beta \sin\Gamma \qquad (22)$$

equations .

$$P(\xi, \beta, \eta) = P_s(\xi, \beta) + P_1(\xi, \beta)[\eta-1] + P_2(\xi, \beta)[\eta^2 - 1] \quad (10)$$

$$v(\xi, \beta, \eta) = v_s(\xi, \beta) + v_1(\xi, \beta)[\eta-1] \quad (11)$$

where

$$P_1(\xi, \beta) = \frac{\psi_s u_s k_\xi}{h_\beta}$$

$$v_1(\xi, \beta) = -\frac{\psi_s v_s}{h_\beta \cos\Gamma}(K_\xi + K_\beta)$$

$$P_2(\xi, \beta) = -\frac{\psi_s v_s \tan\Gamma}{2h_\beta}(K_\xi + K_\beta) \quad (12)$$

in which subscript s indicates values just behind the shock. Most of the details for derivation of Eqs.(10-11), and assumptions used for this purpose are given in Ref. 16. Some of these assumptions are that velocity component w is zero throughout the shock layer, curvilinear coordinate (ξ,β,η) is strictly orthogonal ,$u \approx u_s$, $v \approx v_s$, $w \approx w_s$, and $B \approx 1$. It is noted that Eqs. (10-11) are approximate, however, they can be explicitly used to calculate p and v along the lines normal to the shock, i.e. η variable lines at constant ξ and β. For calculation of shock values p_1, p_2 and v_1 in relations (12) the shock geometry should be known; this will be introduced later.

Having calculated p at each point along an η variable line, other thermodynamic properties of ρ and h can be evaluated using isentropic relations for a perfect gas. In fact at each point, η and therefore ψ is known; see Fig. 5. Since the flow is isentropic along the streamlines, thermodynamic properties at each point are related to their values just behind the shock for the same ψ; these include ρ,T and enthalpy $\hat{h}$. The other component of velocity , u, would be calculated knowing that the total enthalpy is constant , i.e.

$$H = \hat{h} + \frac{1}{2}(u^2 + v^2) = H_\infty \quad (13)$$

The other important equation that is obtained by integrating Eq. (6) is

$$n_b - \frac{n_b^2 K_\beta}{2} = \frac{\psi_s}{h_\beta}\int_0^1 \frac{dn}{\rho u} \quad (14)$$

Using this equation , n_b, the normal distance between the shock and the calculated body (where $\psi = 0$) is computed at each ξ and β . This distance is along η variable line towards the body.

Shock geometry

Based on the suggestion of VanDyke and Gordon [17], shock surface produced by a longitudinal conic-section body shape can also be described by a conic - section. Using this idea the three-dimensional shock surface in the subsonic-transonic region can be represented by three longitudinal conic-sections blended in the circumferential direction with an ellipse as

$$r = f(x, \phi) \quad (15)$$

where $f(x, \phi)$ is defined as

$$f^2\left[\tilde{B}(x)\cos^2\phi + \sin^2\phi\right] + f\tilde{C}(x)\cos\phi = \tilde{D}(x) \quad (16)$$

in which

$$\tilde{B}(x) = \frac{f_2^2}{f_1 f_3}$$

$$\tilde{C}(x) = \tilde{B}(x)(f_3 - f_1)$$

flow. Therefore, if $F(x, r, \phi) = r - f(x, \phi) = 0$, then the unit vector $\hat{e}_n$ would be

$$\hat{e}_n = \frac{-\nabla \vec{F}}{|\nabla \vec{F}|} \qquad (2)$$

Unit vectors $\hat{e}_\xi$ and $\hat{e}_\beta$ are tangent to the shock surface and are so chosen that $\hat{e}_\xi$ would be in the direction of tangential velocity, and $\hat{e}_\beta$ is perpendicular to $\hat{e}_\xi$ and $\hat{e}_n$, i.e. $\hat{e}_\beta = \hat{e}_n \times \hat{e}_\xi$. The velocity vector in shock coordinate system is defined as,

$$\vec{V} = u\hat{e}_\xi + v\hat{e}_n + w\hat{e}_\beta \qquad (3)$$

in which u, v, and w are velocity components. Based on the definition of $\hat{e}_\xi$ and $\hat{e}_\beta$, the crossflow velocity component at the shock, w_s, would be zero. It is noted that this curvilinear coordinate system is not orthogonal within the three-dimensional shock layer. For thin shock layers, however, orthogonality can be assumed in the outer inviscid region of shock layer (i.e. excluding boundary layer). Transformations between curvilinear, cylindrical, and cartesian coordinate systems must be available to complete the analysis. Details of these transformations are given in Ref. 16, and will not be discussed here.

Stream functions

According to Ref. 15, two stream functions ψ and Φ are such defined that $\rho\vec{V} = \vec{\nabla}\psi \times \vec{\nabla}\Phi$ Substitution of this relation in continuity equation, and rewriting this equation in curvilinear coordinate system yields [12]

$$\rho u h_\beta \, B = \frac{\partial \psi}{\partial \beta}\frac{\partial \Phi}{\partial n} - \frac{\partial \psi}{\partial n}\frac{\partial \Phi}{\partial \beta}$$

$$\rho v h_\xi \, h_\beta \, AB = \frac{\partial \psi}{\partial \xi}\frac{\partial \Phi}{\partial \beta} - \frac{\partial \psi}{\partial \beta}\frac{\partial \Phi}{\partial \xi}$$

$$\rho w h_\xi \, A = \frac{\partial \psi}{\partial n}\frac{\partial \Phi}{\partial \xi} - \frac{\partial \psi}{\partial \xi}\frac{\partial \Phi}{\partial n} \qquad (4)$$

in which ρ is density, h_ξ and h_β are scale factors in ξ and β directions respectively, and A and B are geometric factors given by

$$A = 1 - nK_\xi \qquad B = 1 - nK_\beta \qquad (5)$$

where k_ξ and k_β répresent curvatures of the shock surface in ξ–n and ξ–β planes, respectively. For a blunt body at hypersonic speeds it can be assumed that with a good approximation w = 0 in the outer inviscid layer [14,15]. This assumption is satisfied if Φ be a function of β, e.g. $\Phi = \beta$. In this case, the last equation in (4) is satisfied and for ψ we would have

$$\frac{\partial \psi}{\partial n} = -\rho v h_\beta B \qquad (6)$$

$$\frac{\partial \psi}{\partial \xi} = \rho v h_\xi \, h_\beta \, AB \qquad (7)$$

Pressure equation

The momentum equation for steady inviscid flow is

$$\vec{V} \cdot \nabla \vec{V} = -\frac{1}{\rho}\vec{\nabla} p \qquad (8)$$

inwhich p is pressure. Again rewriting this equation in curvilinear coordinate system of (ξ,β,n), and assuming w=0 , the momentum equation in direction normal to the shock , i.e. n, becomes [12]

$$\frac{u}{A}\left(\frac{1}{h_\xi}\frac{\partial v}{\partial \xi} + uk_\xi\right) + v\frac{\partial v}{\partial n} = -\frac{1}{\rho}\frac{\partial p}{\partial n} \qquad (9)$$

Euations (6,7) and (9) are the governing equations for the outer inviscid flow in the shock layer. Without discussing any details, by defining a new coordinate system of (ξ,β,η) where $\eta = \frac{\psi}{\psi_s}$, the two following important equations can be obtained from these

boundary layer. Using boundary layer analysis at stagnation point and on a flat plate, relations can be obtained for determination of convective heat transfer coefficient, C_H, as a function of boundary layer edge properties and wall temperature, T_w. Fortunately, these relations can be modified for axisymmetric flow, and if the body is at angle of attack or it has a non symmetric geometry, they can still be modified to determine C_H along streamlines on the surface of body [1-5].

From the above discussion it is clear that the solution of inviscid flow not only is needed for calculation of C_H, but also is required for determination of streamilne paths on the surface of body [3,6,7]. Although numerical solution of Euler equations are more economical than that of N.S. equations, they are still not fast enough. Various approximate engineering methods have been developed to calculate distributions of pressure, temperature, and velocity components on the surface of body [8-13]. All of these engineering methods, that solve Euler equations approximately, are essentially based on Refs. 14 and 15. The first step in the procedure of these inverse methods is to assume a shock wave for the body at hypersonic flow. Flowfield calculation starts right behind the shock wave and will be ended where the stream function ψ becomes equal to zero. The surface with $\psi=0$ defines a calculated body for the assumed shock wave. Based on the error between geometry of calculated and real bodies , a new shock wave is introduced. Calculation procedure is repeated until the computed body matches the real one. To make the calculation faster, such an iterative procedure is only applied to subsonic-transonic portion of the inviscid flowfield, and for the supersonic portion a marching method is used in which the shock wave is modified step by step.

In this paper, using an approximate engineering method, inviscid flow is solved around a number of hyperonic noses, and their results for subsonic-transonic region are compared with other numerical results and experimental data. In all cases excellent agreement is observed. These results include flowfields behind a parabolic shock wave, around a spherical nose at zero angle of attack. around a parabolic body at angle of attack, and around an elliptic cone at angle of attack.

2-Analysis

As stated in previous section, inviscid flow is solved using an inverse method, therefore it is needed to define an initial 3D shock geometry. This geometry is introduced in a cylindrical coordinate, as $r=f(x,\phi)$. According to the views of shok geometry, shown in Figs. 1 and 2, angles of $\Gamma(x,\phi)$ and $\delta_\phi(x,\phi)$ are defined as

$$\tan \delta_\phi = \frac{1}{f}\frac{df}{d\phi} \qquad (1)$$

$$\sigma = \phi - \delta_\phi$$

$$\tan \Gamma = \frac{df}{dx}\cos\delta_\phi$$

In these figures, $\hat{e}_x$, $\hat{e}_r$, $\hat{e}_\phi$, are unit vectors of cylindrical coordinate. Note that in axisymmetric flow $\delta_\phi = 0$. The shock oriented coordinate of (ξ, β, n), to which the Euler equations will be transferred is introduced in Figs. 3 and 4. According to these figures, ξ and β represent coordinates of a point on the shock, and n would be the normal distance from this point towards inside the shock. Such a coordinate system, which is co-centered with cylindrical coordinate, is suitable for the analysis of thin shock layer in hypersonic

Approximate Solution of Inviscid Flow Around the Nose of Hypersonic bodies At Angle of Attack

S.M.H.Karimian
AssociateProfessor

A.Mehdizadeh
Research Assistant

Aerospace Engineering Deptartment,
Amirkabir University of Technology

Abstract

Aerodynamic heating calculation of a hypersonic body is normally performed during the critical part of its flight trajectory. This requires solution of inviscid flowfield around the hypersonic body and most crucially around its nose, for several times. In this paper, using Thin-Shock-Layer theory, three-dimensional Euler equations are transferred to a shock-oriented coordinate, and by implementing appropriate approximations, an inverse method is applied for the calculation of flowfield between the shock wave and the body surface. Based on the nose shape of a hypersonic body flying at M_∞ a three-dimensional shock geometry is first estimated. Using explicit formulations obtained from the inverse method, inviscid flowfield behind the shock wave is numerically calculated. From this calculation the resulted surface with zero stream function corresponds to a nose that has produced the estimated shock wave. Based on the error between this nose and the real one, the 3D shock shape is repeatedly changed until the calculated nose matches the real one. Using this engineering approximate method, which is very fast, all of the flow variables can be determined in the solution domain. An excellent agreement is observed between the results obtained in this paper and those calculated by others or extracted from experiment. Since the method is very fast it can be used for preliminary design, or parametric study of vehicle aerodynamics and thermal protection at hypersnoic flows. Such a fast method is also desirable for making initial conditions suitable for CFD codes.

Keywords

Inviscid Hypersonic Flow, Approximate Solution, Inverse Method, Aerodynamic Heating, Thin Shock Layer

1-Introduction

Since Aerodynamic Heating is a function of V_∞^3, its consideration in hypersonic flights is more important than that of aerodynamic forces. Therefore in high speeds the first concern is the large amount of heat production on the surface of vehicle which highly increases the shell temperature. One way to calculate this shell temperature is to solve viscous flow equations around the body and heat balance equation within the shell, simultaneously. At the present, solution of 3D viscous flow equations around a hypersonic vehicle, or even its nose, at angle of attack is expensive and very time consuming. If such a calculation was needed only once, the cost and time were not a major problem. However, the difficulty is that shell temperature should be calculated during parts of flight trajectory for several times.

The method often used is to split the flowfield into two regions of viscous flow in boundary layer and inviscid flow outside the